engineering proceedings

MDPI

Proceeding Paper

Improved Virtual Synchronous Generator-Based Control Scheme for Enhanced Transient Response in Microgrids †

Mandarapu Srikanth and Yellapragada Venkata Pavan Kumar *

School of Electronics Engineering, VIT-AP University, Amaravati 522237, Andhra Pradesh, India; srikanth.20phd7032@vitap.ac.in

* Correspondence: pavankumar.yv@vitap.ac.in; Tel.: +91-863-2370155

† Presented at the 4th International Electronic Conference on Applied Sciences, 27 October–10 November 2023; Available online: https://asec2023.sciforum.net/.

Abstract: Synchronous generator-based power stations, with their inherent inertia, can maintain frequency stability during sudden load switching, while distributed generating station-driven microgrids suffer from a lack of natural inertia. Cascaded power, voltage, and current controllers are a widespread control strategy used to regulate the power output of distributed generating stations to maintain frequency and voltage within stable limits. Virtual synchronous generator (VSG) control for the power controller is used as a potential solution to emulate inertia. To derive maximum benefit from VSG, proper tuning of its multiple parameters is required. In this direction, earlier works proposed the equivalence between the droop and VSG schemes, which suggested that the droop coefficient value could be directly used in the design of VSG. As an improvement to these conventional works, the proposed work in this paper identifies that VSG delivers a better response when an equalizing constant is used to adjust the droop coefficient value than using it directly. This paper proposes implementing the VSG with an equalizing constant as a new design parameter. A description of designing the parameters of this improved VSG considering the equalizing constant is also discussed in this paper. The performance of the conventional VSG and the proposed improved VSG are compared. From the results, it is observed that, at load switching, the output frequency of the proposed method in all test cases has settled at less than 3 s, while the conventional method took a maximum of 6 s in critical cases. Further, the output frequency's maximum peak with the proposed method is 3 Hz less than the conventional method. These, along with other metrics, validate the importance of the proposed improved VSG-based control scheme for the enhancement of transient responses in microgrids.

Keywords: frequency stability; microgrids; transient response; virtual synchronous generator

Citation: Srikanth, M.; Kumar, Y.V.P. Improved Virtual Synchronous Generator-Based Control Scheme for Enhanced Transient Response in Microgrids. *Eng. Proc.* **2023**, *56*, 4. https://doi.org/ 10.3390/ASEC2023-15390

Academic Editor: Simeone Chianese

Published: 27 October 2023

1. Introduction

To provide uninterrupted and quality electricity, distributed generating sources are located near local loads. By interconnecting smaller-capacity distributed generation stations (DGSs) together, the concept of microgrids has emerged [1]. Most DGSs use power electronics converters to connect the source and load. These power electronics-driven DGSs, due to their smaller capacity, cannot help improve the transient response from inherent inertia [2]. This led to the development of virtual inertia techniques using power controllers. Four varieties of virtual inertia emulation schemes are available in the literature. They are (a) droop control [3], (ii) Synchronverter [4], (iii) current-controlled virtual synchronous generator (VSG) [5], and (iv) voltage-controlled VSG [6]. Among these, voltage-controlled VSG exhibits better transient response in both island and grid-connected modes. A typical layout of the microgrid with a VSG-based power controller is shown in Figure 1. These VSG controllers, by emulating virtual inertia, improve frequency stability in both transient and steady-state conditions. Even though the stability of frequency is guaranteed during

steady-state, the response during the transient stage may take a longer time to settle. This may lead to unnecessary tripping caused by the frequency relay with its definite time delay setting. Therefore, a study to modify the conventional VSG control to reduce the chances of unnecessary tripping in microgrids is essential.

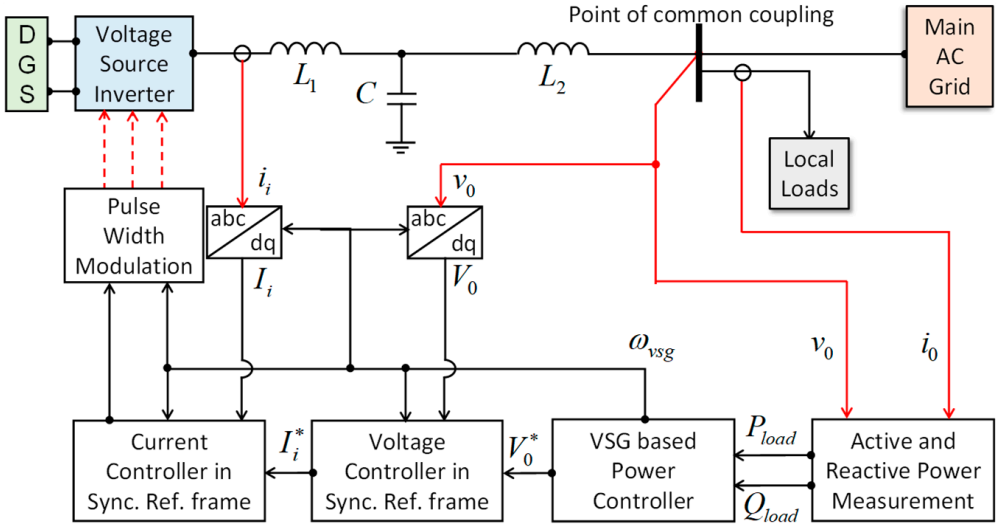

Figure 1. Typical layout of a single DGS-based microgrid with a VSG-based multiloop control scheme.

To analyze the issue, studying the impact of VSG parameters on stability and response is crucial. Stability analysis of voltage-controlled VSG through small signal modeling considering parameter changes is covered in [7]. Literature suggests that adjusting the VSG's inertia coefficient enhances transient response, with [8] presenting newer methods for this. However, these bring longer computation times and insufficient results [9]. Through the comparison between active power loops of droop control and VSG control, ref. [10] identifies the relation between the speed governor proportional gain constant ($K_{p\text{-}\omega}$) as the inverse of active power—frequency (P-ω) droop coefficient (D_p). In [9], adjusting $K_{p\text{-}\omega}$ in the VSG setup is recommended for enhanced performance, but without a specified process. This study reveals that using an equalizing factor to modify $K_{p\text{-}\omega}$ reduces unwarranted tripping during significant load shifts. A procedure for designing this improved VSG (MVSG) control using the equalizing factor is detailed here. Simulations under diverse load conditions validate the effectiveness of the proposed approach in improving transient performance.

The remaining sections of the paper are organized as follows: Section 2 describes the conventional VSG. Section 3 presents the proposed MVSG. Section 4 analyzes the results obtained by simulating the proposed scheme at various load conditions. Finally, the conclusions of the proposed work are discussed in Section 5.

2. Conventional Virtual Synchronous Generator

A VSG will emulate virtual inertia that is similar to the inertia of traditional synchronous generators by making use of electrical energy storage systems. This improves stability under transient conditions. The swing equation of the conventional synchronous generator (1), which is translated into an algorithm, is used for developing an active power loop in the VSG. Where P^* is the equivalent of reference mechanical power input, P_{load} is the electrical power output, J is the equivalent of rotor inertia, D is the damping constant, ω_o is the nominal angular frequency, which normally is equivalent to 50 Hz, and ω_{vsg} is the rotor speed estimated by the VSG.

$$P^* - P_{load} - D(\omega_{vsg} - \omega_0) = J\omega_0 \frac{d\omega_{vsg}}{dt} \quad (1)$$

In the conventional synchronous generator scheme, P^* indicates the reference mechanical power input to the conventional synchronous generator that is provided by a speed governor. In literature, this is mimicked with P-ω droop control. The control equation of this droop control is given in (2), where P_0 is the nominal value of active power and P_{load} is the measured value of active power delivered to the load. Substituting P^* in (1) with that in (2), the resulting equation is shown in (3). Similarly, the reactive power loop is designed for VSG based on (4), where v_0^* and v_{load} are the reference voltage to the voltage controller and voltage measured at the load terminals, respectively; Q_0 and Q_{load} are the nominal values of reactive power and reactive power measured at the load terminals, respectively; and $K_{q\text{-}v}$ is the droop gain coefficient of conventional reactive power–voltage (Q-v) droop control. In this conventional VSG, the relation between $K_{p\text{-}\omega}$ and D_P is maintained as $K_{p\text{-}\omega} = 1/D_P$.

$$P^* = P_0 - K_{p-\omega}(\omega_{vsg} - \omega_0) \tag{2}$$

$$P_0 - K_{p-\omega}(\omega_{vsg} - \omega_0) - P_{load} - D(\omega_{vsg} - \omega_0) = J\omega_0 \frac{d\omega_{vsg}}{dt} \tag{3}$$

$$v_0^* = v_{load} - K_{q-v}(Q_0 - Q_{load}) \tag{4}$$

3. Proposed Modified VSG and Design of its Parameters

From the guidelines and the control parameters of the VSG that are provided in [9–11], the procedure for designing the $K_{p-\omega}$ of proposed MVSG, as shown in Figure 2, is consolidated as follows: With a maximum allowable active power variation $\Delta P_{\max}$ of 62.8 $\times 10^3$ W and a maximum allowable frequency deviation of 2%, the value of D_p is calculated as shown in (5).

$$D_p = \frac{\Delta P_{\max}}{\Delta \omega_{\max}} = \frac{62.8 \times 10^3}{(2 \times \pi \times 50) \times 2\%} = 1 \times 10^{-4} \tag{5}$$

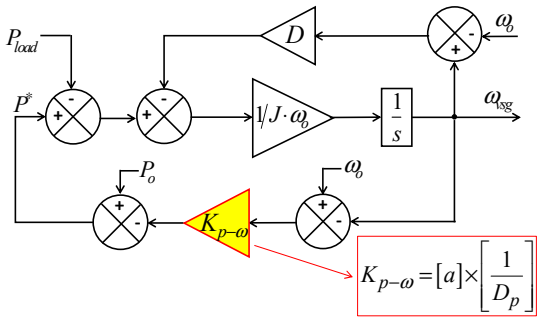

Figure 2. Active power loop structure of the proposed MVSG.

With a maximum allowable reactive power variation $\Delta Q_{\max}$ of 21.02 $\times 10^3$ Var, the base value of the apparent power is obtained as given in (6).

$$S_{base} = \sqrt{(\Delta P_{\max})^2 + (\Delta Q_{\max})^2} = \sqrt{(62.8 \times 10^3)^2 + (21.02 \times 10^3)^2} = 66.224 \times 10^3 \text{ VA} \tag{6}$$

For $K_{p-\omega} = 20pu$, its equivalent value is evaluated by solving (7).

$$K_{p-\omega} = 20pu = 20 \times \frac{S_{base}}{\omega_0} = [a] \times \left[\frac{1}{D_p}\right] \tag{7}$$

With a nominal frequency of 50 Hz in $\omega_o = 2 \times \pi \times 50 = 314.7\ rad/s$, '$a$' is an equalizing constant whose value is obtained as shown by (8).

$$\therefore 20 \times \frac{66.224 \times 10^3}{314.7} = [a] \times \left[\frac{1}{1 \times 10^{-4}}\right] \Rightarrow a = 2.3759 \quad (8)$$

A distinction in the active power loop structures between the conventional VSG and the proposed MVSG is apparent from Figure 2, in relation to the constant 'a'. In conventional VSG, this value is held at 1, whereas for the proposed MVSG, it is set at 2.3759.

4. Simulation Results and Comparative Analysis

A single DGS-based microgrid system feeding two three-phase loads and connected to the utility grid at 440 V and 50 Hz is considered in this study. The total system is modeled in MATLAB. The inverter's output is regulated by two control methodologies.

- Conventional methodology: traditional VSG scheme (with a = 1) [10].
- Proposed methodology: MVSG (with a = 2.3759).

Load-1 is of a fixed and continuous type with 1200 W + j300 Var, whereas Load-2 is characterized as a momentary load occurring between 80 and 100 s. The transients linked with the activation and deactivation of Load-2 at 80 s and 100 s are denoted as T80 and T100, respectively. The loadings with Load-2 during test cases 1, 2, and 3 are 3000 W, 5000 W, and 10,000 W, respectively. Table 1 presents the specific values of various control parameters associated with MVSG.

Table 1. Control parameters of MVSG.

Parameter	Description	Value
J	Equivalent rotor inertia (kg-m^2)	56.3
ω_o	Nominal angular frequency (rad/s)	314.7
$K_{p-\omega}$	Active power loop gain (pu)	20
D	Damping coefficient (pu)	17
K_{q-v}	Reactive power loop gain	1.48×10^{-3}

In test case 1, corresponding to T80, both methods brought the frequency below 51 Hz before 83 s, indicating stability. However, the conventional VSG method performed worse due to a smaller gap between the system frequency and 51 Hz at 83 s, as observed in Figure 3. In contrast, the proposed MVSG method showed better results. Similar findings applied to T100, with both methods lifting the frequency above 49 Hz before 103 s for stability. Again, the conventional VSG method had a weaker transient response than the proposed MVSG method, owing to smaller frequency deviations at 103 s (Figure 3a). In test case 2, using the proposed MVSG, the frequency reached stability below 51 Hz before 83 s (T80) and above 49 Hz before 103 s (T100). However, with conventional VSG, the frequency almost reached 51 Hz at 83 s (T80) and nearly 49 Hz at 103 s (T100), pushing the system towards instability. This is evident in the zoomed views of T80 and T100 in Figure 3b.

In test case 3, the system frequency with conventional VSG stayed above 51 Hz at 83 s and below 49 Hz at 103 s under T80 and T100, indicating instability (Figure 3c). In contrast, the proposed MVSG ensured stability with a good transient response during T80 and T100. The active power results under this test case 3 are shown in Figure 4a. From this, it is noticed that the conventional method exhibits a longer settling time than the proposed method. Further, from the voltage results, as noticed in Figure 4b and Table 2, for T80 and T100 transients, conventional VSG had a longer settling time (about 5 s) than the proposed MVSG. Table 2 outlines a thorough comparison of both methods' transient performance under various test cases involving frequency and voltage aspects, showcasing the best-performing method.

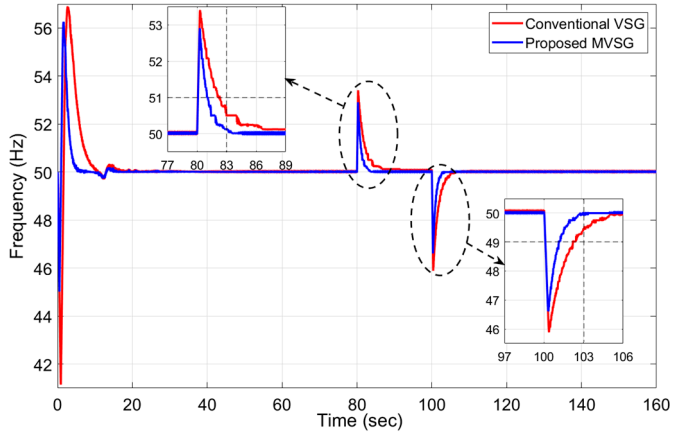

(**a**) Test case 1.

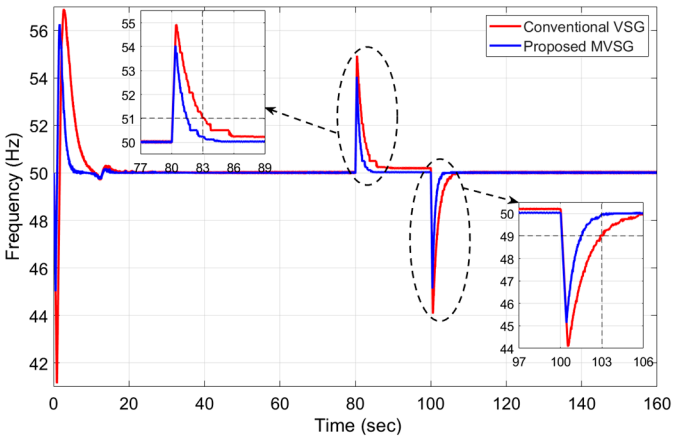

(**b**) Test case 2.

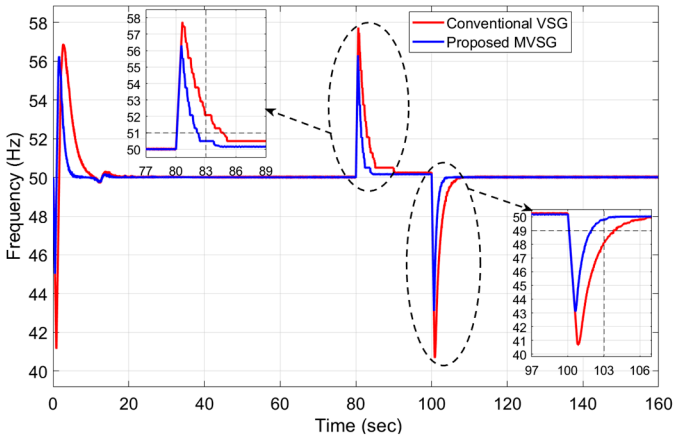

(**c**) Test case 3.

Figure 3. Frequency responses obtained with various test cases.

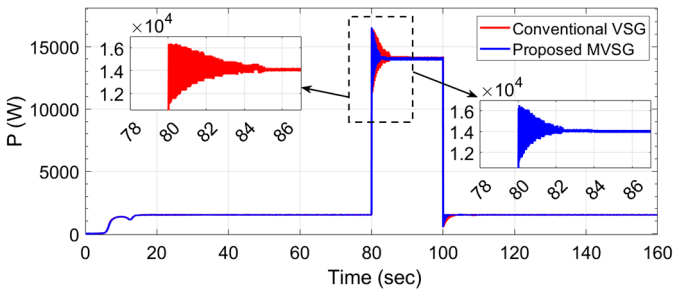

(**a**) Active power response.

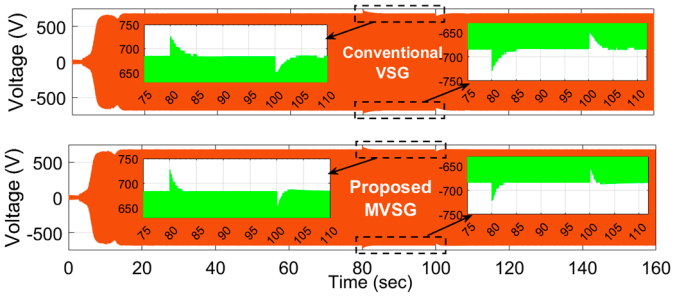

(**b**) Voltage response.

Figure 4. Active power and voltage profiles observed under test case 3.

Table 2. Comparison of conventional and proposed methods in various performance aspects.

Performance Parameter	Test Cases	T80				T100			
		Aspect	I—Conv. VSG [10]	II—Prop. MVSG	Best Method	Aspect	I—Conv. VSG [10]	II—Prop. MVSG	Best Method
Frequency characteristics	Case-1	Maximum peak (Hz)	53.4	52.9	II	Maximum peak (Hz)	45.9	46.6	II
	Case-2		54.8	54	II		44.2	45.2	II
	Case-3		57.7	56.3	II		40.8	43.2	II
	Case-1	Freq. at 83 s (Hz)	50.5	50.2	II	Freq. at 100 s (Hz)	49.5	50	II
	Case-2		51	50.2	II		49	50	II
	Case-3		52.1	50.5	II		48.1	49.8	II
	Case-1	Settling time (s)	91.6	83.2	II	Settling time (s)	105	102	II
	Case-2		85.9	84.2	II		106	103	II
	Case-3		90.2	50.3	II		106	103	II
Voltage characteristics	Case-1	Maximum peak (Volts)	696	696	I and II	Maximum peak (Volts)	667	667	II
	Case-2		709	709	I and II		658	661	II
	Case-3		726	727	I and II		645	650	II
	Case-1	Settling time (s)	2.9	1.4	II	Settling time (s)	2.6	1.8	II
	Case-2		3.7	1.8	II		4.5	2.1	II
	Case-3		5	2.3	II		5	2.4	II

5. Conclusions

From Table 2, it is found from test case 3 that the conventional VSG scheme took around 5 s to come down below the allowable limit of 51 Hz. This made the system vulnerable to unnecessary tripping. Based on a detailed study on the design of MVSG and the impact of various parameters on the transient performance, it is identified that an equalizing factor, 'a' plays a vital role in improving the stability and response. Conventional VSG utilizes '$a = 1$' in the design of VSG. From a critical understanding of the design of the VSG, it is identified that '$a = 2.3759$' is the appropriate value that should be used in the design of the MVSG for the system parameters considered in this work. This MVSG scheme performance in test case 3 has caused the frequency to come below the allowable limit in 2.2 s, which is less than the 3 s time delay. In terms of frequency settling time, the proposed MVSG method has outperformed the conventional VSG method. The superiority of the proposed method is further confirmed in test case 3 through a lesser frequency dip than the conventional method.

Author Contributions: Conceptualization, M.S.; methodology, Y.V.P.K.; software, Y.V.P.K.; formal analysis, M.S.; funding acquisition, Y.V.P.K.; investigation, M.S.; resources, Y.V.P.K.; data curation, M.S. and Y.V.P.K.; supervision, Y.V.P.K.; validation, Y.V.P.K.; visualization, M.S.; project administration, Y.V.P.K.; writing—original draft, M.S.; writing—review and editing, Y.V.P.K. All authors have read and agreed to the published version of the manuscript.

Funding: This research received no external funding.

Institutional Review Board Statement: Not applicable.

Informed Consent Statement: Not applicable.

Data Availability Statement: Not applicable.

Conflicts of Interest: The authors declare no conflict of interest.

References

1. Srikanth, M.; Venkata Pavan Kumar, Y. A State Machine-Based Droop Control Method Aided with Droop Coefficients Tuning through In-Feasible Range Detection for Improved Transient Performance of Microgrids. *Symmetry* **2022**, *15*, 1. [CrossRef]
2. V. Pavan Kumar, Y.; Bhimasingu, R. Electrical Machines Based DC/AC Energy Conversion Schemes for the Improvement of Power Quality and Resiliency in Renewable Energy Microgrids. *Int. J. Electr. Power Energy Syst.* **2017**, *90*, 10–26. [CrossRef]
3. Soni, N.; Doolla, S.; Chandorkar, M.C. Improvement of Transient Response in Microgrids Using Virtual Inertia. *IEEE Trans. Power Deliv.* **2013**, *28*, 1830–1838. [CrossRef]
4. Dong, S.; Chen, Y.C. Adjusting Synchronverter Dynamic Response Speed via Damping Correction Loop. *IEEE Trans. Energy Convers.* **2017**, *32*, 608–619. [CrossRef]
5. Mo, O.; D'Arco, S.; Suul, J.A. Evaluation of Virtual Synchronous Machines with Dynamic or Quasi-Stationary Machine Models. *IEEE Trans. Ind. Electron.* **2017**, *64*, 5952–5962. [CrossRef]
6. D'Arco, S.; Suul, J.A.; Fosso, O.B. A Virtual Synchronous Machine for Distributed Control of Power Converters in SmartGrids. *Electr. Power Syst. Res.* **2015**, *122*, 180–197. [CrossRef]
7. Song, Z.; Zhang, J.; Tang, F.; Wu, M.; Lv, Z.; Sun, L.; Zhao, T. Small Signal Modeling and Parameter Design of Virtual Synchronous Generator to Weak Grid. In Proceedings of the 2018 13th IEEE Conference on Industrial Electronics and Applications (ICIEA), Wuhan, China,, 31 May–2 June 2018; IEEE: Piscataway, NJ, USA, 2018; pp. 2618–2624.
8. Hou, X.; Sun, Y.; Zhang, X.; Lu, J.; Wang, P.; Guerrero, J.M. Improvement of Frequency Regulation in VSG-Based AC Microgrid Via Adaptive Virtual Inertia. *IEEE Trans. Power Electron.* **2020**, *35*, 1589–1602. [CrossRef]
9. Liu, J.; Miura, Y.; Ise, T. Comparison of Dynamic Characteristics Between Virtual Synchronous Generator and Droop Control in Inverter-Based Distributed Generators. *IEEE Trans. Power Electron.* **2016**, *31*, 3600–3611. [CrossRef]
10. Wu, H.; Ruan, X.; Yang, D.; Chen, X.; Zhao, W.; Lv, Z.; Zhong, Q.-C. Small-Signal Modeling and Parameters Design for Virtual Synchronous Generators. *IEEE Trans. Ind. Electron.* **2016**, *63*, 4292–4303. [CrossRef]
11. Meng, X.; Liu, J.; Liu, Z. A Generalized Droop Control for Grid-Supporting Inverter Based on Comparison Between Traditional Droop Control and Virtual Synchronous Generator Control. *IEEE Trans. Power Electron.* **2019**, *34*, 5416–5438. [CrossRef]